



Evolving strain partitioning in the Eastern Himalaya: The growth of the Shillong Plateau



Yani Najman^{a,*}, Laura Bracciali^{a,b}, Randall R. Parrish^b, Emdad Chisty^{c,1}, Alex Copley^d

^a Lancaster Environment Centre, Lancaster University, LA1 4YQ, UK

^b NERC Isotope Geoscience Laboratory, BGS Keyworth, NG12 5GG, UK

^c Cairn Energy, 50 Lothian Road, Edinburgh, EH3 9BY, UK

^d Dept of Earth Sciences, Cambridge University, Downing St, Cambridge, CB2 3EQ, UK

ARTICLE INFO

Article history:

Received 5 May 2015

Received in revised form 6 October 2015

Accepted 11 October 2015

Available online xxxx

Editor: A. Yin

Keywords:

Shillong Plateau uplift

Indo–Burman Ranges

Brahmaputra palaeo-drainage

Eastern Himalaya

Surma Basin evolution

Bangladesh

ABSTRACT

The Shillong Plateau is the only raised topography (up to 2000 m elevation) in the Himalayan foreland. It is proposed to have had a major influence on strain partitioning and thus tectonics in the Eastern Himalaya. Additionally, its position on the trajectory of the summer monsoon means it has influenced the regional climate, with reduced erosion rates proposed over geological timescales in its lee. The timing of surface uplift of the plateau has been difficult to determine. Exhumation rates have been calculated over geological timescales, but these seem at variance with estimates based upon extrapolating the present day velocity field measured with GPS, and it has thus been suggested that exhumation and surface uplift are decoupled. We determine the timing of surface uplift using the sedimentary record in the adjacent Surma Basin to the south, which records the transition from a passive margin with southward thickening sedimentary packages to a flexural basin with north-thickening strata, due to loading by the uplifting plateau. Our method involves using all available 2D seismic data for the basin, coupled to well tie information, to produce isochore maps and construct a simple model of the subsidence of the Surma basin in order to assess the timing and magnitude of flexural loading by the Shillong Plateau. We conclude that the major period of flexural loading occurred from the deposition of the Tipam Formation (3.5–~2 Ma) onwards, which is likely to represent the timing of significant topographic growth of the Shillong Plateau. Our isochore maps and seismic sections also allow us to constrain the timing of thinning over the north–south trending anticlines of the adjacent basin-bounding Indo–Burman Ranges, as occurring over this same time interval. The combined effect of the uplift of the Shillong Plateau and the westward encroachment of the Indo–Burman Ranges to this region served to sever the palaeo-Brahmaputra drainage connection between Himalayan source and Surma Basin sink, at the end of Tipam Formation times (~2 Ma).

© 2015 Elsevier B.V. All rights reserved.

1. Introduction

The Shillong Plateau is a unique feature, being the only raised topography (up to 2000 m elevation) in the Himalayan foreland (Fig. 1). It consists of Precambrian Indian plate basement, partially overlain by Cretaceous and Cenozoic sediments in the south, east and west. To the south the plateau is juxtaposed against the adjacent Surma Basin along the Dauki Fault. The plateau is variously proposed to be: i) a pop-up structure, bounded by two reverse faults, the Dauki Fault to the south and the Oldham Fault to the

north (Bilham and England, 2001; Islam et al., 2011); ii) the result of uplift through the mechanism of the Oldham Fault as a backthrust to the Dauki Fault interpreted as a north-dipping thrust (Yin et al., 2010); or iii) the Oldham fault as a backthrust to a master blind north-dipping fault at depth, with the “Dauki Fault” as the surface expression of a fold axial trace propagating from this fault (Clark and Bilham, 2008). Biswas et al. (2007) consider the degree of importance of the Oldham Fault to the evolution of the Plateau to be minor, and propose the Dauki Fault to be the major structure responsible for the plateau's uplift.

Representing a major deviation in geometry to the otherwise simplistic Himalayan arc (Bendick and Bilham, 2001), the Shillong Plateau has had a major influence on strain partitioning in the Eastern Himalaya, affecting the seismic risk in the surrounding re-

* Corresponding author.

E-mail address: y.najman@lancs.ac.uk (Y. Najman).

¹ Current address: Santos Sangu Field Ltd, Dhaka, Bangladesh.

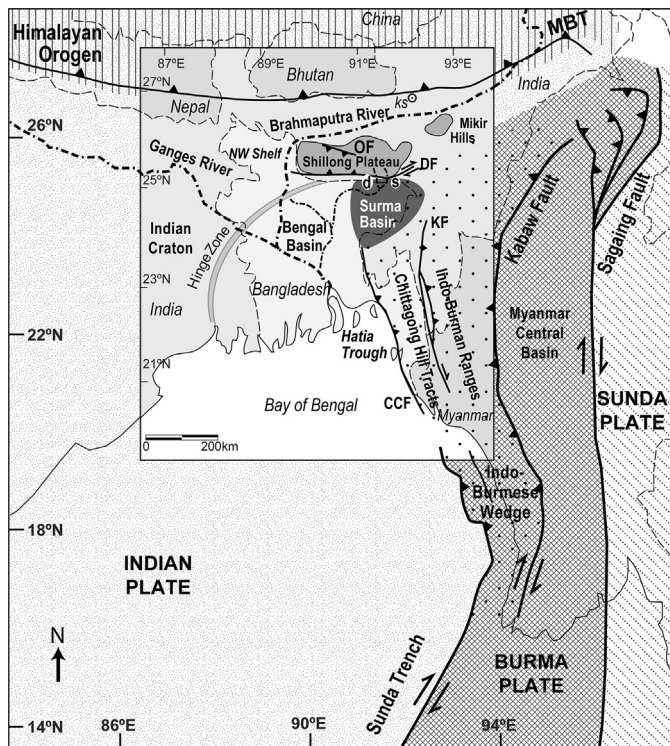


Fig. 1. Schematic geological map of the Indo-Burman region in Eastern Asia showing the Indian, Burma and Sunda Plates and the location of the Surma Basin, Shillong Plateau and Indo-Burman Wedge (dotted area) that includes the Indo-Burman Ranges and Chittagong Hill Tracts. National boundaries and main drainages of the Ganges and Brahmaputra Rivers are also shown. d and s: Dauki and Shari Rivers draining the Shillong Plateau. DF: Dauki Fault; OF: Oldham Fault; KF: Kaladan Fault; CCF: Chittagong Coastal Fault; ks: location of the Kameng section consisting of Siwalik sediments of Chirouze et al. (2013) as discussed in text. Redrawn after Najman et al. (2012) and Maurin and Rangin (2009). Boxed area is the region shown in Fig. 6.

gions (e.g. Banerjee et al., 2008; Bilham and England, 2001). The onset of its exhumation may have been responsible for potentially coeval kinematic changes such as the initiation of E–W extension in central Tibet, eastward expansion of high topography in Tibet, onset of crustal rotation of crustal fragments in SE Tibet and re-establishment of eastward subduction beneath the Indo-Burman ranges (Clark and Bilham, 2008).

Located on the trajectory of the Indian Summer Monsoon, the plateau perturbs the regional distribution of precipitation, and its southern flank is the wettest place on earth (Bookhagen and Burbank, 2010). Grujic et al. (2006) proposed that temporal and spatial variation in erosion rates in Bhutan were the result of climatic modulation in the rain shadow of the uplifting Shillong plateau, a hypothesis later questioned by e.g. Adlakha et al. (2013). By contrast, others proposed that such variations in Bhutan reflected variable strain partitioning due to the plateau's exhumation (Adams et al., 2015; Biswas et al., 2007; Coutand et al., 2014). It has also been proposed that the plateau's uplift has had a major influence on the strain partitioning effects between the Indian and Sunda plate, expressed in the evolution of the Indo-Burman Ranges (IBR) (Maurin and Rangin, 2009). The uplift of the plateau combined with the western propagation of the IBR was then responsible for major alterations in the palaeo-Brahmaputra drainage in the hydrocarbon producing region of the adjacent Surma Basin which lies to the south of the plateau and west of the IBR (Fig. 1).

Understanding when surface uplift of this plateau occurred is key to understanding events such as the proposed climate-tectonic couplings. Exhumation of the plateau has been inferred from bedrock low-temperature thermochronometry data to have occurred between 15–9 Ma (Biswas et al., 2007; Clark and Bilham,

2008). However, there is little constraint to the timing of surface uplift, or whether Miocene exhumation/cooling of the crystalline bedrock of the Plateau coincided with surface uplift; indeed the two have been proposed to be decoupled (Biswas et al., 2007). Previously proposed estimates for the timing of surface uplift range from Early Miocene (Yin et al., 2010) through Pliocene (Johnson and Alam, 1991) to Quaternary (Ferguson et al., 2011). We bring a new approach to the problem. We use seismic and well data from the Surma Basin to construct isochore maps for the Neogene Formations of the Surma Basin. The recorded flexural thickening of the sediments is a result of changes in load at the margin of the basin. From this information, we construct a simple model of the subsidence of the Surma Basin in order to assess the timing and magnitude of flexural loading by the Shillong Plateau, and so use the stratigraphy to infer the tectonic history of the region. Thus we provide a new source of information that has a fundamentally different sensitivity to bedrock thermochronology, and allows differentiation between signals resulting from surface uplift versus those which may be the result of exhumation balanced by erosion, with no net surface uplift occurring.

2. Previous constraints to the timing of Shillong Plateau evolution

The northern part of the plateau is devoid of sedimentary cover and preserves old paleo-erosion surfaces and pre-Cenozoic apatite (U–Th)/He and fission track ages (Biswas et al., 2007). This clearly demonstrates no significant burial in the Cenozoic. Conversely, thermochronological bedrock data indicate clear evidence of burial heating during the Cenozoic for the southern part of the plateau under a thick sedimentary cover, followed by initiation of exhumation of the plateau sometime between 15 and 9 Ma as inferred by both apatite (U–Th–[Sm])/He and apatite fission track (AFT) dating (Biswas et al., 2007; Clark and Bilham, 2008). Biswas et al. (2007) proposed that the plateau's surface uplift could have been chronologically decoupled from its exhumation due to the different erodibilities of the plateau's basement and draping cover sediments, with surface uplift initiated when basement exhumed to surface, any time after 3.5–5.5 Ma.

Sedimentological constraints from the Cenozoic sediments draping the southern part of the plateau, and their equivalents in the adjacent Surma Basin to the south, have also been used to constrain the evolution of the plateau. The Surma Basin (Fig. 1) is bounded to the north by the Shillong Plateau, to the east by the north–south trending folds of the westward propagating Indo-Burman Ranges (IBR), to the west by the Indian craton, and to the south the basin is open to the Bay of Bengal. The basin contains 16–18 km of Cenozoic sediment overlying the likely-transitional Indian crust (Alam et al., 2003; Ghatak and Basu, 2011). The stratigraphy (Fig. 2) consists of Eocene marine facies (Sylhet and Kopili Formations), Oligo-Miocene marine-deltaic facies of the Barail Formation and overlying Surma Group (Bhuban and Bokabil Formations), overlain by the Pliocene Tipam Formation and Pleistocene Dupil Tila Formations, the latter both of fluvial facies (Reimann, 1993). Recently, the stratigraphy and dating of the depositional ages of the Neogene Surma Basin deposits has been updated with their grouping into seismic megasequences (MS; Najman et al., 2012 Fig. 2). Seismic megasequence MS1 (corresponding to the Bhuban and Bokabil Formations) lacks any continuous lithological marker horizons and is predominantly composed of deltaic deposits. The top of MS1 is regionally marked by the Upper Marine Shale, a 70 m thick marine shelfal mudstone. The homogeneous seismic package that characterises the lower part of MS2 corresponds to the massive and lithologically uniform sandstones of the braided fluvial Tipam Formation. This is overlain by the more heterogeneous seismic package of the Dupi Tila

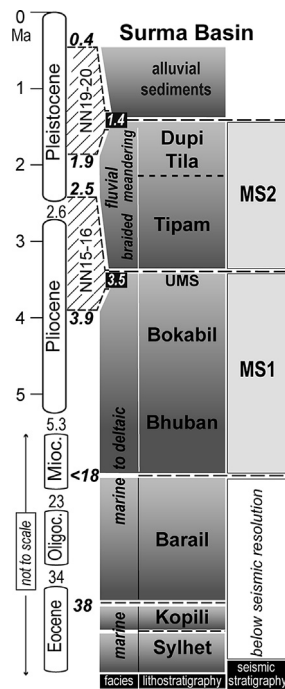


Fig. 2. Schematic stratigraphy of the Surma Basin. The stratigraphic boundaries are constrained with variable degree of confidence by biostratigraphy, magnetostratigraphy, and detrital mineral dates, as detailed in Najman et al. (2012) and Bracciali et al. (2015), and references therein. MS: Megasequence; NN: nannoplankton zones. UMS = Upper Marine Shale.

Formation (alternating fluvial-channel sandstones and flood-plain silty-clay deposits of meandering fluvial facies). MS3, the uppermost megasequence unit, is absent in the Surma Basin, where the Dupi Tila Formation is overlain by Holocene alluvial sediments.

Previous work has focused on the time when the Surma Basin changed from a passive margin with sedimentary units thickening south, to a flexural basin, with sediment units thickening north, interpreted to be due to loading from the adjacent uplifting Shillong Plateau. Uddin and Lundberg (2004) constructed isochore maps for the Bhuban and Bokabil Formations from well log data and compared the data to the Bouguer anomaly data for the region. In spite of discrepancies in the calculations of thickness for the Bhuban Formation between their work and ours (for a number of wells, the value they quote for the base of the Bhuban Formation is the number we calculate for the total depth of the well, which did not necessarily penetrate to the stratigraphic base of the Bhuban in all cases), their work, like the present work, records thickening of basin fill to the south. By comparison with gravity anomaly data for the region, they conclude the major subsidence must have therefore occurred post Bokabil deposition.

Johnson and Alam (1991) noted northward thickening in post-Miocene strata (their Fig. 6), but did not differentiate whether such thickening commenced in the Pliocene Tipam Formation or overlying Pleistocene Dupi Tila Formation. They suggested that the plateau uplift which induced this change in sediment thickness distribution began in Tipam rather than Dupi Tila Formation times based on the arguments that: 1) the plateau is draped by Miocene but not Plio-Pleistocene strata and 2) the Tipam Formation in the Surma Basin shows a marked increase in sedimentary lithic fragments compared to underlying formations, interpreted as reflecting recycling from the plateau's sedimentary cover due to the uplifting of the plateau at this time. However, the lack of Plio-Pleistocene sediments atop the plateau may simply reflect their erosion subsequent to uplift, and neither our previous study (Bracciali et al., 2015) nor that of Uddin and Lundberg (1998) replicated the petrographic data showing increased sedimentary lithic fragments ob-

served in the Tipam Formation, as recorded by Johnson and Alam. Furthermore, we argue that the Tipam Formation was not eroded from the sedimentary cover of the uplifting Shillong Plateau, which would presumably have been the Surma Group, given a) mineral grain size broadly shows an increase from the Surma Group to the Tipam Formation and b) the continuation in the trend of youngest detrital rutile U–Pb dates decreasing in age upsection from the Surma Group to the Tipam Formation (Bracciali et al., 2015, their Fig. 2). This trend reflects the continued exhumation to progressively deeper levels of the Himalayan source region (Bracciali et al., 2015), as expected when derived directly from a rapidly exhuming orogen. Thus it is proposed that the Tipam Formation was derived directly from the Himalaya, not recycled from the Himalayan-derived Surma Group deposited atop the Shillong Plateau.

We therefore consider that northward thickening of sedimentary units indicating flexural loading due to thrusting on the southern margin of the Shillong Plateau has not, thus far, been constrained more precisely than “post Bokabil Formation times”.

3. Our approach; constraints on timing of Shillong Plateau uplift and Indo–Burman Range propagation

As outlined above, we use seismic and well data to construct isochore maps of the Surma Basin formations. We then use the data to construct a simple model of the subsidence of the Surma Basin in order to assess the timing and magnitude of flexural loading by the Shillong Plateau.

3.1. Isochore maps for Surma Basin formations

New regional seismic horizons (Intra-Dupi Tila; Base Dupi Tila [Top Tipam]; Base Tipam [Top Bokabil]; Base Bokabil [Top Bhuban]; Base Bhuban [Top Barail]) were created from all seismic data (2D) available to Cairn Energy (Edinburgh, UK), with well data (well tops, stratigraphic markers, Drill Stem Test results) used to create well to seismic ties. For depth conversion, all available checkshot data from the Surma Basin area and its surroundings were analysed. The Titas-11 well checkshot data approximates the average checkshot data for the wells of the area, hence the 2nd order polynomial curve of Titas-11 checkshot was used for the regional time-depth conversion as follows:

$$\text{Depth} = 0.0003071 \cdot (\text{TWT}) \cdot 2 + 0.77364 \cdot (\text{TWT}) + 1.0458.$$

Surface time grids and contours were depth-converted using the polynomial equation determined for this purpose. Respective fault files were used while creating the time and depth grids. No smoothing was used for surface time contours, but surface depth and thickness contours were smoothed.

The maps were prepared using the software application Petrosys after exporting seismic horizons picked in the IESX software application of Geoframe. A 500 m by 500 m cell size was used for creating grids in Petrosys. Final maps (Fig. 3) were prepared using the Petrosys interactive mapping module. A 50 ms contour interval was used for time (surface and thickness) maps, while 100 m was used for depth (surface and thickness/isochore maps). Thickness maps were prepared using thickness grids and contours, which were created using the top and base grids of the formations.

The two significant features of the resulting maps are:

1) The Surma Group sediments, both Bhuban and Bokabil Formations, thicken south. By contrast, the Tipam Formation does not thicken to the south, but maintains a relatively constant north-south thickness throughout the basin. By inference, the “post-Miocene” northward thickening as recorded first by Johnson and Alam (1991) is now tightly constrained as post-Tipam. Such variations are also well illustrated when viewing individual north-south

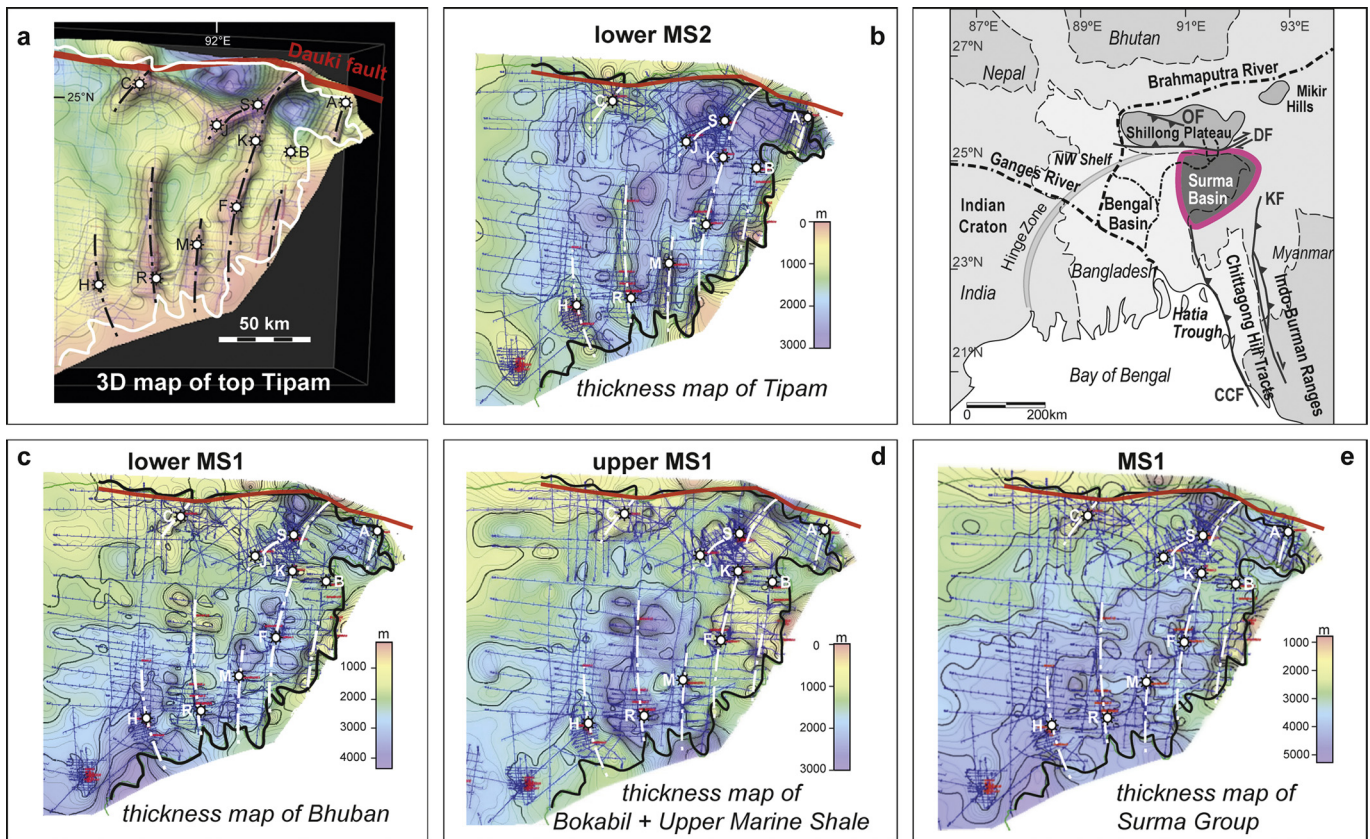


Fig. 3. Subsurface maps of the Surma Basin, as located on the map in Fig. 1 and upper right panel of this figure (Surma Basin highlighted by red line). a) 3D subsurface map of the Top Tipam reflector (by depth), showing the ~N–S anticlines formed in relation to the frontal deformation zone of the IBR. Dashed lines represent anticline axes. Main boreholes in the area are located with the following abbreviations: C: Chhatak; H: Habiganj; R: Rashidpur; J: Jalalabad; S: Sylhet; M: Moulavi Bazar; F: Fenchuganj; K: Kailastita; B: Beani Bazar; A: Atgram. The international border between Bangladesh and India and the approximate position of the Dauki Fault are also represented as a white and a red line, respectively. b) to e) 2D subsurface seismic-derived isochore maps of cumulative sediment thickness (by depth); national border of Bangladesh represented as a black line). Traces of N-trending anticlines as in (a) are located to aid comparison. The north-trending anticline structures correspond to thickness variations in the Tipam Formation (b), and are superimposed on a relatively constant north–south thickness throughout the basin. Conversely, thickness maps (c) to (e) show a marked thickening towards the south of the basin and lack any spatial relation between the distribution of thickness and the location of anticlines, indicating that beginning of folding is syn-Tipam in age. Note that: i) a lower number of well tie correlations were employed for the Bhuban Formation map compared to the Bokabil Formation map because not all wells penetrated to base Bhuban; ii) the apparent thinning to the east in the Bhuban and Bokabil maps is highly questionable and most probably an artefact due to poor well control coupled with poor seismic imaging at the eastern extent of the area of study.

seismic lines (e.g. Fig. 4). These thickness variations are interpreted to reflect the transition from a passive margin to a flexural basin, resulting from loading by the uplifting Shillong Plateau.

2) Thinning of strata over the north–south trending anticlines, indicative of the westward propagation of the IBR to this outermost region, is of syn-Tipam age. This a) corroborates previous studies from more limited seismic datasets (e.g. Johnson and Alam, 1991; Sikder and Alam, 2003) and b) spatially extends the studies of Maurin and Rangin (2009) and Najman et al. (2012) who noted similar ages for the timing of folding in more southern regions of the outermost western IBR and Chittagong Hill Tracts (CHT; an extension of the IBR).

3.2. Flexural modelling

In order to relate the changes in the sedimentary architecture in the Surma Basin to the tectonics of the Shillong Plateau, we undertook flexural modelling of the basin. In order to reduce the complexity of the models we restricted our analysis to a N–S striking profile. This modelling therefore ignores the effects of the Indo–Burman Ranges. However, because this range is propagating westwards into the basin, the resulting flexure results in no changes in N–S dips or thickness contrasts. Therefore, by only examining N–S striking profiles, we can isolate the effects of the tectonics of the Shillong Plateau and the subsidence in the Surma

Basin. We constructed a simple model that includes the effects of southwards-increasing subsidence due to either thermal effects or sediment loading in the Bengal Basin, and also flexural loading of the region of the Surma Basin by thrusting on the southern margin of the Shillong Plateau. We used the long-established model for the flexure of an elastic plate overlying an inviscid substrate. Based upon the analysis of gravity anomalies, we assume an elastic thickness of 30 km for the Indian plate (e.g. McKenzie et al., 2014). This value is consistent with the flexure beneath the Ganges foreland basin and the relationship between topography and gravity in the southern part of the Indian plate, so we assume it applies to all of the Indian lithosphere. The thrusting on the southern margin of the Shillong Plateau is modelled as a load on the end of a broken elastic plate. The resulting equations represent a damped sinusoid (e.g. see Turcotte and Schubert (2002) for a derivation) as have been applied to the region, for example by Lyon-Caen and Molnar (1983) and McKenzie and Fairhead (1997). We use this straightforward approach rather than a more complex back-stripping method in order to capture the main features of the stratigraphy with the simplest model that can encapsulate the major aspects of the stratigraphy and constrain the timing of loading on the margin of the Surma Basin.

In the following analysis we assumed that all beds were deposited at close to sea level, and fill the available accommodation space, consistent with the fluvial and deltaic depositional envi-

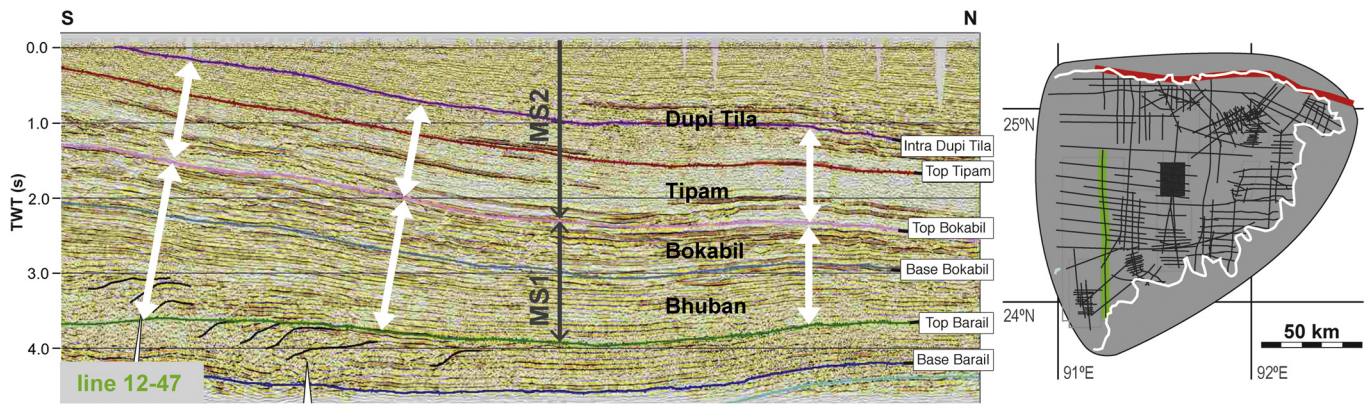


Fig. 4. Example seismic section from the Surma Basin. Right panel: Location map of seismic line within the Surma Basin; grey shaded area corresponds to the Surma Basin as located in Fig. 1. The seismic network of Bangladesh (black thin lines) used to derive the thickness maps of Fig. 3 is shown as a reference. The international border between Bangladesh and India and the approximate location of the Dauki Fault are represented as a white and a red line, respectively. The seismic N–S section (left panel) shows a marked increase in thickness towards the south in the Base Bhuban (= Top Barail) to Top Bokabil package, vs. the constant thickness of the Base Tipam (= Top Bokabil) to Intra Dupi Tila package. Megasequences MS1 and MS2 are indicated, as well as interpreted regional horizons.

ronments of the sediments. The key aspects of the stratigraphy that we aim to reproduce in these models are: (1) the thickening to the south in the Bhuban and Bokabil Formations; (2) the roughly constant thickness of the Tipam Formation; (3) the thickening to the north in post-Tipam times as seen in the package of sediment comprising the combined Dupi Tila Formation and overlying Holocene units; (4) the roughly horizontal dip of the Bhuban and Bokabil Formations in the central part of the basin, overlain by north-dipping Tipam and Dupi Tila beds. The thickening to the south in the Bhuban and Bokabil Formations implies subsidence due to thermal effects or sediment loading in the Bengal Basin. We model this process as a simple linearly-increasing subsidence from north to south, with the amount of subsidence prescribed to match the thicknesses of the units. In this situation, the Bhuban and Bokabil Formations have the geometry shown in Fig. 5 – lower panel. This is the model stratigraphy immediately before the deposition of the Tipam Formation begins at ~ 3.5 Ma.

In contrast to the Bhuban and Bokabil Formations, the Tipam Formation does not show significant N–S thickness changes, implying that a further source of subsidence must be present in order to balance the thickening to the south seen in the underlying units. This subsidence can be modelled as the onset of flexural loading in the region of the Shillong Plateau. The wavelength of flexure based on our assumed elastic thickness of 30 km (McKenzie et al., 2014) is similar to that observed due to the southwards-increasing subsidence in the Bhuban and Bokabil Formations, meaning that the Tipam Formation can be deposited with a roughly constant thickness (Fig. 5 – middle panel). The amount of loading required to balance the southwards-increasing subsidence is discussed below.

The northwards thickening and northwards dip of the combined Dupi Tila Formation and overlying Holocene sediments requires that the amount of flexural subsidence relating to loading in the Shillong Plateau increases above that present during the deposition of the Tipam Formation, equivalent to additional overthrusting of the southern margin of the Shillong Plateau over the margin of the Surma Basin (Fig. 5 – upper panel). The amount of flexure required to produce the degree of northwards thickening seen in the combined Dupi Tila + Holocene units sedimentary package has the additional effect of altering the dips of the underlying units, so that the boundaries of the Bokabil and Bhuban Formations, which had southwards dips in the centre of the basin, become flatter and are overlain by more recent sediments dipping to the north, as seen on the seismic sections (e.g. Fig. 4).

Although this modelling has neglected the secondary effects of compaction and minor faulting within the basin, it reproduces the major first-order features of the stratigraphy. The comparison be-

tween the model results and the Surma Basin stratigraphy suggests that the Shillong Plateau began to exert a significant load on the margin of the Surma Basin, and produced a flexural basin, during the deposition of the Tipam Formation (3.5– ~ 2 Ma). This load then continued to grow during the deposition of the Dupi Tila Formation and younger units.

The total load that is required to produce the model sedimentary geometry shown in Fig. 5 is 1.4×10^{12} N/m along-strike, if the load is treated as a vertical mass emplaced on the end of an elastic plate. This value can be compared with an independent estimate of the mass imposed on the margin of the Surma Basin by the overthrusting of the Shillong Plateau. Throughout the ~ 17 km thickness of the Surma Basin sequence, thrusting on the margin of the range juxtaposes crystalline basement in the hanging wall of the Dauki Fault against the basin sediments. The higher density of the basement means that this fault motion will apply a load to the basin. Additionally, the topography at the surface also results in a load being applied to the basin margin. Assuming an average density difference of 300 kg/m^3 between the sediments and the basement, that the basement has a density of 2800 kg/m^3 , and that the Plateau has overthrust the basin by 18 km (equivalent to a 45 degree dip of the Dauki Fault), we can estimate the total load to be 1.2×10^{12} N/m along-strike. The 0.2×10^{12} N/m difference between this value and that calculated from the basin stratigraphy is insignificant, given the assumptions regarding sediment and basement density and the dip of the Dauki Fault. This comparison demonstrates that the stratigraphy in the Surma Basin is consistent with flexural subsidence due to loading by thrusting on the margin of the Shillong Plateau, which initiated during the deposition of the Tipam Formation (3.5– ~ 2 Ma) and was focused during the subsequent deposition of the Dupi Tila Formation and younger units.

4. Discussion

4.1. Exhumation and uplift of the Shillong Plateau

Our proposal for the timing of initiation of significant loading, which is likely to represent active thrusting and substantial surface uplift of the Shillong Plateau during Tipam Formation times (ca 3.5 to 2 Ma) fits well with the work of Vernant et al. (2014). Using GPS, they estimate horizontal shortening on the southern margin of the Shillong Plateau of 3 mm/yr in the west, increasing to 7 mm/yr in the east. At these rates, it would only take

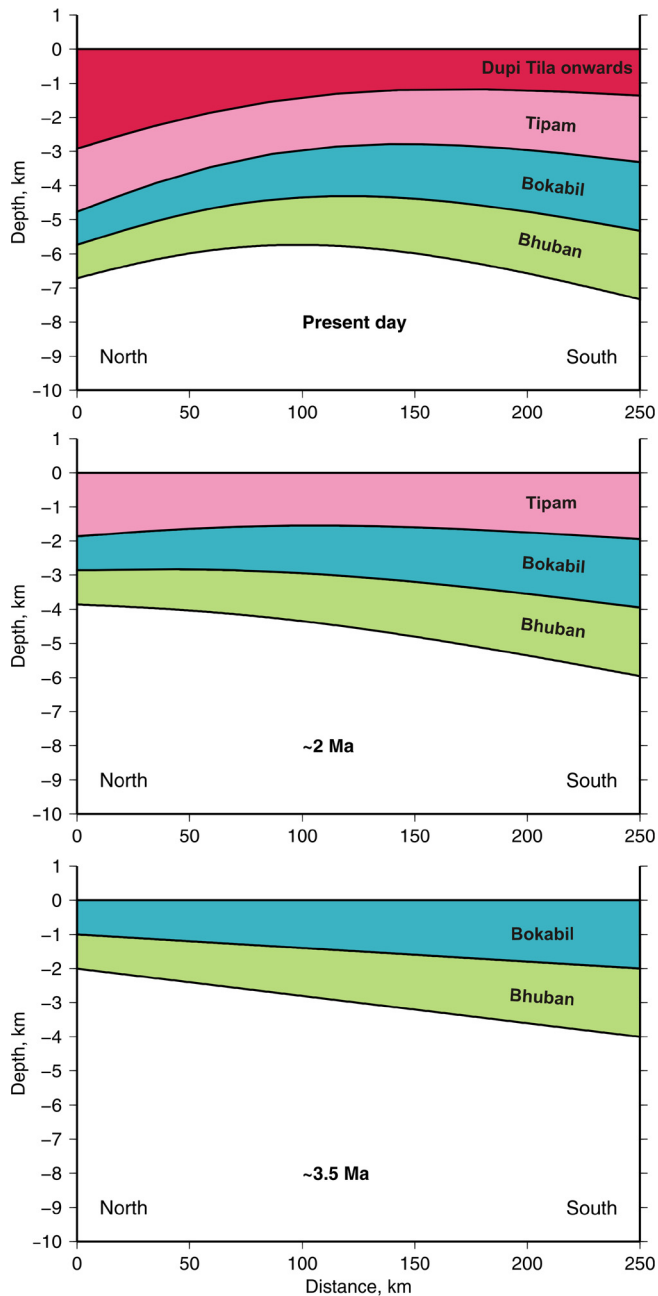


Fig. 5. Lower panel: model stratigraphy at ~ 3.5 Ma, following deposition of the Bokabil and Bhuban Formations in a basin with subsidence increasing to the south. Middle panel: model stratigraphy at ~ 2 Ma, when the onset of flexural loading by the Shillong Plateau has balanced the southwards thickening due to the basin subsidence evident before ~ 3.5 Ma. Top panel: present day model stratigraphy, following the flexural loading by the Shillong Plateau. The lower units thicken to the south, and have sub-horizontal dips in the centre of the basin. The upper units thicken north, and dip north. The Tipam formation is transitional, has a roughly constant thickness, and marks the onset of flexural loading by the Shillong Plateau. See text for details.

a few Ma to produce the total offset on the Dauki Fault (i.e. the basin sediment thickness plus the plateau height). This is consistent with the time our sedimentological data imply the thrusting started, but inconsistent with the average vertical faulting rate as determined from geological exhumation rates (Clark and Bilham, 2008). Vernant et al. (2014) propose that the apparent discrepancy can be explained if the present day convergence across the Dauki Fault is considerably faster today compared to the average rate over the past 10 My. They suggest that such an increase occurred in order to keep total convergence rate between India and

central Tibet constant whilst a co-incident decrease of convergence rate is recorded in Bhutan (McQuarrie et al., 2014).

Biswas et al. (2007) suggested that exhumation and surface uplift could have been decoupled, achieved due to the contrasting erodibilities of the Shillong Plateau Precambrian basement and its overlying sedimentary cover, which predominantly consists of Cenozoic Himalayan-derived sediment. In this proposal, conversion of rock uplift into surface uplift occurred only when the more resistant basement became exposed, which they calculated occurred sometime after 3.5–5.5 Ma. Regarding the time of exposure and subsequent erosion of basement, it should be noted that although sediment from the Shari and Dauki rivers draining the Shillong Plateau today (Fig. 1) is 100% basement-derived, as evidenced by mica Ar–Ar and zircon fission track ages which are all pre-Cenozoic (Najman et al., 2008, see also Biswas et al., 2007 for plateau bedrock zircon U–Th–[Sm]/He data), this was not the case even as late as Dupi Tila times (<2 Ma). Analyses of the Pleistocene Dupi Tila Formation, deposited by rivers draining the Shillong Plateau (Section 4.3) document detrital rutile U–Pb ages, detrital mica Ar–Ar ages and detrital zircon fission track ages all with significant Himalayan-aged Cenozoic populations (56%, 89% and 92% of totals, respectively) (Bracciali et al., 2015; Najman et al., 2005), indicative of erosion from the plateau's Himalayan-sourced sedimentary cover rather than its basement. This indicates that significant erosion of the exposed basement occurred only recently, in agreement with present day plateau topography where only the southern flank is incised.

The published bedrock thermochronological data (Biswas et al., 2007; Clark and Bilham, 2008) indicate that a maximum of 3 km of sediment has been stripped of the southern Shillong plateau since ~ 10 Ma, with a period of late Miocene cooling likely the result of a degree of sediment stripping at that time. By contrast, predominantly Cretaceous ages are recorded north of the Oldham Fault. The following scenarios to explain the combination of published bedrock data and our new data, are examined below:

The Dauki Fault, bounding the southern margin of the plateau, can be interpreted as an originally rift-related passive margin fault (Ferguson et al., 2011), reactivated due to the Shillong's increasing proximity to the Himalaya. Initiation of rapid movement of the Dauki Fault in Pliocene times, as demonstrated by our data, resulted in rise of significant topography and basin loading beginning at 3.5– ~ 2 Ma, coinciding with emergence from marine conditions and terrestrial sedimentation in the Surma Basin.

Regarding the plateau's earlier, Miocene, history, in one scenario, the southern plateau's Miocene bedrock thermochronology may be explained as the result of flexural uplift of the Indian plate associated with a peripheral forebulge. Later, on nearing the Himalayan front, the bounding normal fault failed, leading to the fault's rapid movement, in a thrust sense, in the Pliocene. We note that the length scale over which the thermochronological data varies between the northern and southern regions of the plateau is considerably shorter than typical forebulge wavelengths; movement on the intervening Oldham Fault may have perturbed the original profile. In an alternative scenario, Miocene bedrock cooling of the southern plateau may have resulted from earlier slow reverse movement on the Dauki Fault. Slow thrust fault motion in the interior of the Indian plate is inferred at the present day from GPS data (Banerjee et al., 2008) and Holocene surface ruptures (Copley et al., 2014). In this model, an increase in the rate of faulting in recent times could be caused by the evolving stress state as the Shillong Plateau approaches the Himalayan front. The net compressive force being transmitted through the plate, and the flexural stresses related to the underthrusting of India beneath Tibet, both involve spatial variations (laterally and vertically), which will affect the rate of motion on a fault that is transported through this stress field. In both the above scenarios, only a minor proportion

of the total sediment stripped off the southern plateau between Miocene and present day, would have been eroded off during the early period of Miocene exhumation.

Finally, we turn to the concept of tectonic-erosion-climate couplings. The uplift of the Shillong Plateau has resulted in the de-

velopment of a rain shadow in its lee in Bhutan. Thus, the region has been used as a case study for the investigation of these inter-relationships. Grujic et al. (2006) proposed that spatial and temporal variations in exhumation rates in Bhutan could be attributed to climatic modulation associated with the Shillong Plateau, although more recently such exhumation dominated by a tectonic influence has been considered more likely (Adlakha et al., 2013; Coutand et al., 2014). We note that if surface uplift of the Shillong Plateau is held responsible for variations in exhumation rate in Bhutan via tectonic-erosion-climate couplings, such rate changes must have occurred post 3 Ma.

4.2. Evolution of the Indo–Burman Ranges

The Indo–Burman Ranges are a westward propagating thrust belt resulting from convergence between the Indian and Sunda plates. The range is divided into the Paleogene Inner Burman Ranges to the east, and Neogene Outer Burman Ranges to the west, separated by the Kaladan Fault. According to Maurin and Rangin (2009), uplift of the Shillong Plateau and rapid westward encroachment of the outermost IBR are integrally linked. Whilst the timing of initiation of the IBR, in the East, is poorly known (estimates range from Late Eocene–Early Oligocene (Mitchell, 1993) to Late Miocene (Ni et al., 1989)), Maurin and Rangin proposed that it was uplift of the Plateau, with consequent deepening and filling of the basin with a large amount of unconsolidated sediment, that facilitated the very rapid, westward propagation of the outer wedge of the IBR since 2 Ma. They proposed, in their study of the strain partitioning between the Indian and Sunda plate, that 2/3 of the parallel to trench component of the strain is accommodated by the Sagaing Fault (Fig. 1), while the remnant oblique strain component is distributed throughout the IBR. They suggested that the progressive westward overprinting of thin-skinned tectonics by thick-skinned tectonics within the IBR was the result of the rapid propagation of the wedge westward. They surmised that this occurred because in order to preserve critical taper and strain partitioning ratios between internal shearing and external shortening, some of the outer zone had to be progressively affected by thick-skinned shear deformation. Our new data with more precise timing for the plateau’s surface uplift and for the westward propagation of the outermost IBR in a region more proximal to the Surma Basin than the study of Maurin and Rangin, upholds their hypothesis in as much as the timing of the two events are broadly synchronous.

4.3. Palaeodrainage of the Brahmaputra River

Establishment of the onset of major surface uplift during Tipam Formation times (3.5–~2 Ma), and westward propagation of the

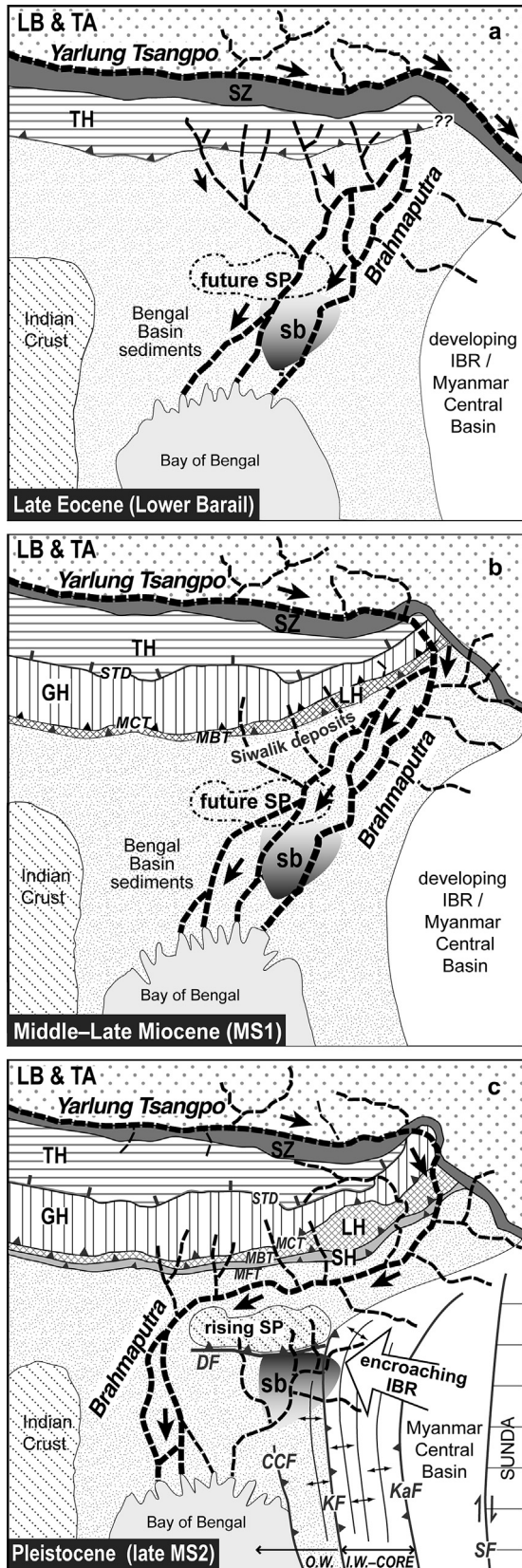


Fig. 6. Model for the Neogene drainage evolution of the Eastern-Himalaya in relation to the tectonic evolution of the region (Ganges drainage not shown). a) Prior to capture by the Brahmaputra, the Yarlung Tsangpo was flowing eastward, likely connected to an eastern Asian river (Robinson et al. 2014), while the Brahmaputra drained the southern slopes of the developing Himalayan orogen. b) After capture in the Early Miocene (Bracciali et al., 2015) and prior to surface uplift of the Shillong Plateau, a very wide Brahmaputra drainage was delivering Transhimalayan Arc-derived (TA in the Asian Lhasa Block, LB) as well as Himalayan-derived detritus to both the Himalayan foreland (e.g. Siwalik deposits) and to the Surma Basin (sb). c) The westward propagation of the IBR towards the rising Shillong Plateau (with surface uplift started during MS2 time as constrained in this work) caused the progressive closure of the eastward route of the Brahmaputra and finally its diversion to the west of the Shillong Plateau. DF, CCF, KF, KaF and SF: Dauki, Chittagong Coastal, Kaladan, Kabaw and Sagaing Fault. Main Himalayan lithotectonics units and their boundaries: SZ: suture zone; TH: Tethyan Himalaya; LH: Lesser Himalaya; SH: Sub-Himalaya; STD: South Tibetan Detachment; MCT: Main Central Thrust; MBT: Main Boundary Thrust; MFT: Main Frontal Thrust. O.W. and I.W.: Outer and Inner Indo–Burmese Wedge (based on Maurin and Rangin, 2009). The ~N trending IBR-related anticlines are also shown. Main thickening trend of the Surma Basin (to the south, panels a and b) or to the north (following flexural loading by the rising Shillong Plateau, panel c) is indicated by a darker shade of grey.

Indo–Burman Ranges to this area in late Tipam times, allows further refinement of the paleodrainage model of the Brahmaputra River. Early workers (Johnson and Alam, 1991) proposed that it was uplift of the Shillong Plateau in the Pliocene that caused diversion of the paleo-Brahmaputra away from the Surma Basin to a new route west of the plateau. A later study (Najman et al., 2012), proposed that it was the encroachment of the IBR against the already uplifted plateau that caused the palaeo-drainage diversion from east to west of the plateau at the time of the Tipam–Dupi Tila transition at ca 2 Ma. Their proposal was based on i) the new thermochronological data of Biswas et al. (2007) and Clark and Bilham (2008) indicating exhumation of the Shillong Plateau in the 15–9 Ma interval, ii) their own ages for propagation of the IBR/CHT south of the Surma Basin at ca 2–3 Ma (Najman et al., 2012), and iii) their own seismic data showing a change in the Surma Basin from a major braid plain to a meandering facies at the Tipam to Dupi Tila Formation transition starting at ca 2 Ma. In our current paper, we concur with the time interval (ca 2 Ma) after which the palaeo-Brahmaputra no longer drained in to the Surma Basin. However, with our improved understanding of both the timing of plateau uplift versus its exhumation, and the timing of IBR encroachment in the immediate vicinity of the Surma Basin, we consider the severance of the palaeo-Brahmaputra drainage route to the Surma Basin to be the result of the combination of both the emerging Plateau surface uplift and westward encroachment of the IBR after this time (Fig. 6c). Thus, at ~2 Ma, the major palaeo-Brahmaputra braid plain (Tipam Formation) no longer drained in to the Surma Basin. Instead, sedimentation in the basin continued with the meandering facies of the Dupi Tila Formation, sourced predominantly by recycling of Himalayan-derived material from the sedimentary cover of the rising plateau immediately to the north.

Cina et al. (2009) and Chirouze et al. (2013) recorded a typical palaeo-Brahmaputra signature (aka Transhimalayan arc-derived detritus) in foreland basin Siwalik Group sediments of latest Miocene age (~7–3 Ma) in the Kameng sedimentary section, Arunachal Pradesh (Fig. 1). From this, and considering the timing of onset of the Shillong Plateau's exhumation between 15–9 Ma, Chirouze et al. (2013) suggested that uplift of the Shillong Plateau may have pushed the paleo-Brahmaputra, already flowing along the Brahmaputra valley, north towards the Himalayan front at this time. Our interpretation of the onset of significant surface uplift of the Shillong Plateau <3.5 Ma can be reconciled with these data by either a) proposing a paleo-Brahmaputra river shifting across its very wide drainage basin extending from foreland basin to Surma Basin, prior to Shillong Plateau uplift (Fig. 6b) or (b) proposing that early exhumation produced subtle topography sufficient to extend the influence of the drainage basin further north-west. Ongoing work, utilising the Siwalik sedimentary record in the lee of the Shillong Plateau in Bhutan will provide constraint to the timing of initial stages of plateau uplift (Govin et al., 2015).

5. Conclusions

Southward thickening of the sedimentary packages in the Surma Basin, typical of passive margin deposition, ceased at the end of Bokabil Formation deposition (3.5 Ma). From then on (Tipam Formation to present day) there is a gradual change to northward thickening of the succession, indicative of deposition in a flexural basin which formed as a result of loading from the adjacent Shillong Plateau's uplift. These data, and the subsequent flexural modelling which utilised this dataset, indicate that significant surface uplift of the Shillong Plateau commenced 3.5–~2 Ma, during deposition of the Tipam Formation. Westward propagation of the Indo–Burman Ranges also occurred in this area at this time, as evidenced by thinning of Tipam strata over the Indo–Burman

anticlines. Thus we consider that the combined influence of the uplifting plateau and westward propagating Indo–Burman Ranges together resulted in the rerouting of the palaeo-Brahmaputra away from the Surma Basin by the end of Tipam Formation deposition (~2 Ma). This is consistent with seismic facies data which show a change from major braid plain deposition during Tipam Formation deposition to meandering facies of the overlying Dupi Tila Formation. Furthermore, we note that previously discussed tectonic–climate couplings illustrated by the proposed synchronicity between Shillong Plateau uplift and decreased erosion rates in the Bhutanese Himalaya in its lee remains valid only if such erosion rates decreased after 3 Ma.

Acknowledgements

This research was supported by NERC (Natural Environment Research Council, UK) through grants NE/F01807X/1 to Y.N. and NE/F017588/1 to R.R.P. Cairn Energy is thanked for providing resources and expertise to the project. Ed Willett and Rob F.E. Jones, both formerly of Cairn Energy, UK, are thanked for their advice and expertise in seismic data analysis and interpretation, and Peter DeCelles and Djordje Grujic for thought provoking discussion.

References

- Adams, B.A., Hodges, K.V., Whipple, K.X., Ehlers, T.A., van Soest, M.C., Wartho, J., 2015. Constraints on the tectonic and landscape evolution of the Bhutan Himalaya from thermochronometry. *Tectonics* 34, 1329–1347.
- Adlakha, V., Lang, K.A., Patel, R.C., Lal, N., Huntington, K.W., 2013. Rapid long-term erosion in the rain shadow of the Shillong Plateau, Eastern Himalaya. *Tectonophysics* 582, 76–83.
- Alam, M., Alam, M.M., Curray, J.R., Chowdhury, M.L.R., Gani, M.R., 2003. An overview of the sedimentary geology of the Bengal Basin in relation to the regional tectonic framework and basin-fill history. *Sediment. Geol.* 155, 179–208.
- Banerjee, P., Burgmann, R., Nagarajan, B., Apel, E., 2008. Intraplate deformation of the Indian subcontinent. *Geophys. Res. Lett.* 35. <http://dx.doi.org/10.1029/2008GL035468>.
- Bendick, R., Bilham, R., 2001. How perfect is the Himalayan arc? *Geology* 29, 791–794.
- Bilham, R., England, P.C., 2001. Plateau “pop-up” in the great 1897 Assam earthquake. *Nature* 410, 806–809.
- Biswas, S., Coutand, I., Grujic, D., Hager, C., Stockli, D., Grasemann, B., 2007. Exhumation and uplift of the Shillong Plateau and its influence on the eastern Himalayas: new constraints from apatite and zircon (U–Th–[Sm])/He and apatite fission track analysis. *Tectonics* 26, TC6013. <http://dx.doi.org/10.1029/2007TC002125>.
- Bookhagen, B., Burbank, D.W., 2010. Toward a complete Himalayan hydrological budget: spatiotemporal distribution of snowmelt and rainfall and their impact on river discharge. *J. Geophys. Res., Earth Surf.* 115, 2003–2012.
- Bracciali, L., Najman, Y., Parrish, R., Akhter, S.H., Millar, I., 2015. The Brahmaputra tale of tectonics and erosion: Early Miocene river capture in the Eastern Himalaya. *Earth Planet. Sci. Lett.* 415, 25–37.
- Chirouze, F., Huyghe, P., van der Beek, P., Chauvel, C., Chakraborty, T., Dupont-Nivet, G., Bernet, M., 2013. Tectonics, exhumation, and drainage evolution of the eastern Himalaya since 13 Ma from detrital geochemistry and thermochronology, Kameng River Section, Arunachal Pradesh. *Geol. Soc. Am. Bull.* 125, 523–538.
- Cina, S.E., Yin, A., Grove, M., Dubey, C.S., Shukla, D.P., Lovera, O.M., Kelty, T.K., Gehrels, G.E., Foster, D.A., 2009. Gangdese arc detritus within the eastern Himalayan Neogene foreland basin: implications for the Neogene evolution of the Yalu–Brahmaputra River system. *Earth Planet. Sci. Lett.* 285, 150–162.
- Clark, M.K., Bilham, R., 2008. Miocene rise of the Shillong Plateau and the beginning of the end for the Eastern Himalaya. *Earth Planet. Sci. Lett.* 269, 336–350.
- Copley, A., Mitra, S., Sloan, R.A., Gaonkar, S., Reynolds, K., 2014. Active faulting in apparently stable peninsular India: rift inversion and a Holocene-age great earthquake on the Tapti Fault. *J. Geophys. Res., Solid Earth* 119. <http://dx.doi.org/10.1002/2014JB011294>.
- Coutand, I., Whipp, D.M., Grujic, D., Bernet, M., Fellin, M.G., Bookhagen, B., Landry, K.R., Ghalley, S.K., Duncan, C., 2014. Geometry and kinematics of the Main Himalayan Thrust and Neogene crustal exhumation in the Bhutanese Himalaya derived from inversion of multithermochronologic data. *J. Geophys. Res., Solid Earth* 119, 1466–1481.
- Ferguson, E.K., Seeber, L., Akhter, S.H., Steckler, M.S., Biswas, A., Mukhopadhyay, B.P., 2011. The Dauki Fault in NE India: a crustal scale thrust-fold reactivating the continental margin. In: American Geophysical Union Fall Meeting. Abstract #T43D-2401.

- Ghatak, A., Basu, A.R., 2011. Vestiges of the Kerguelen plume in the Sylhet Traps, northeastern India. *Earth Planet. Sci. Lett.* 308, 52–64.
- Govin, G., Najman, Y., Grujic, D., van der Beek, P., Davenport, J., Huyghe, P., 2015. Constraining the timing of Shillong Plateau uplift from a study of the palaeo-Brahmaputra deposits, Siwalik Group, Sandrup Jongkhar, Western Bhutan. In: American Geophysical Union Fall Meeting 2015 (Abstract).
- Grujic, D., Coutand, I., Bookhagen, B., Bonnet, S., Blythe, A., Duncan, C., 2006. Climatic forcing of erosion, landscape and tectonics in the Bhutan Himalayas. *Geology* 34, 801–804.
- Islam, M.S., Shinjo, R., Kayal, J.R., 2011. Pop-up tectonics of the Shillong Plateau in northeastern India: insight from numerical simulations. *Gondwana Res.* 20, 395–404.
- Johnson, S.Y., Alam, A.M.N., 1991. Sedimentation and tectonics of the Sylhet Trough, Bangladesh. *Geol. Soc. Am. Bull.* 103, 1513–1527.
- Lyon-Caen, H., Molnar, P., 1983. Constraints on the structure of the Himalaya from an analysis of gravity-anomalies and a flexural model of the lithosphere. *J. Geophys. Res.* 88, 8171–8191.
- Maurin, T., Rangin, C., 2009. Structure and kinematics of the Indo–Burmese Wedge: recent and fast growth of the outer wedge. *Tectonics* 28, TC2010. <http://dx.doi.org/10.1029/2008TC002276>.
- McKenzie, D., Fairhead, D., 1997. Estimates of the effective elastic thickness of the continental lithosphere from Bouguer and free air gravity anomalies. *J. Geophys. Res.* 102, 523–527.
- McKenzie, D., Yi, W., Rummel, R., 2014. Estimates of T_e from GOCE data. *Earth Planet. Sci. Lett.* 399, 116–127.
- McQuarrie, N., Tobgay, T., Long, S., Reiners, P., Cosca, M., 2014. Variable exhumation rates and variable displacement rates: documenting recent slowing of Himalayan shortening in western Bhutan. *Earth Planet. Sci. Lett.* 386, 161–174.
- Mitchell, A.H.G., 1993. Cretaceous–Cenozoic tectonic events in the western Myanmar (Burma)–Assam region. *J. Geol. Soc.* 150, 1089–1102.
- Najman, Y., Allen, R., Bickle, M., Carter, A., Garzanti, E., Oliver, G., Wijbrans, J., 2005. Bengal Basin, Bangladesh. Final Report. Cairn Energy, Edinburgh, UK (Internal Report).
- Najman, Y., Bickle, M., BouDagher-Fadel, M., Carter, A., Garzanti, E., Paul, M., Wijbrans, J., Willett, E., Oliver, G., Parrish, R., Akhter, S.H., Allen, R., Ando, S., Chisty, E., Reisberg, L., Vezzoli, G., 2008. The Paleogene record of Himalayan erosion: Bengal Basin, Bangladesh. *Earth Planet. Sci. Lett.* 273, 1–14.
- Najman, Y., Allen, R., Willett, E.A.F., Carter, A., Barford, D., Garzanti, E., Wijbrans, J., Bickle, M., Vezzoli, G., Ando, S., Oliver, G., Uddin, M., 2012. The record of Himalayan erosion preserved in the sedimentary rocks of the Hatia Trough of the Bengal Basin and the Chittagong Hill Tracts, Bangladesh. *Basin Res.* 24, 499–519.
- Ni, J.F., Bevis, M., Holt, W.E., Wallace, T.C., Seager, W.R., 1989. Accretionary tectonics of Burma and the three-dimensional geometry of the Burma subduction zone. *Geology* 17, 68–71.
- Reimann, K.-U., 1993. *Geology of Bangladesh*. Borntraeger, Berlin, p. 154.
- Sikder, A., Alam, M., 2003. 2-D modelling of the anticlinal structures and structural development of the eastern fold belt of the Bengal Basin, Bangladesh. *Sediment. Geol.* 155, 209–226.
- Turcotte, D.L., Schubert, G.G., 2002. *Geodynamics*, 2nd edition. Cambridge University Press, Cambridge, UK.
- Uddin, A., Lundberg, N., 1998. Cenozoic history of the Himalayan–Bengal system: sand composition in the Bengal Basin, Bangladesh. *Geol. Soc. Am. Bull.* 110, 497–511.
- Uddin, A., Lundberg, N., 2004. Miocene sedimentation and subsidence during continent–continent collision, Bengal Basin, Bangladesh. *Sediment. Geol.* 164, 131–146.
- Vernant, P., Bilham, R., Szeliga, W., Drupka, D., Kalita, S., Bhattacharyya, A.K., Gaur, V.K., Pelgay, P., Cattin, R., Berthet, T., 2014. Clockwise rotation of the Brahmaputra Valley relative to India: tectonic convergence in the eastern Himalaya, Naga Hills, and Shillong Plateau. *J. Geophys. Res., Solid Earth* 119, 6558–6657.
- Yin, A., Dubey, C.S., Webb, A., Kelty, T.K., Grove, M., Gehrels, G.E., Burgess, W.P., 2010. Geologic correlation of the Himalayan orogen and Indian craton: Part 1. Shillong Plateau and its neighboring regions in NE India. *Structural geology, U–Pb zircon geochronology, and tectonic evolution. Geol. Soc. Am. Bull.* 122, 336–359.